Nitric oxide-dependent cytoskeletal changes and inhibition of endothelial cell migration contribute to the suppression of angiogenesis by RAD50 gene transfer

Hyun Kook, Kyu Youn Ahn, Song Eun Lee, Hee Sam Na, Kyung Keun Kim*

Research Institute of Medical Sciences and Medical Research Center for Gene Regulation, Chonnam National University Medical School, Hak-Dong 5, Dong-Ku, Kwangju 501-190, South Korea

Abstract Previous reports showed that human RAD50 (hRAD50) gene delivery induced regression of an experimental rat tumor and porcine neointimal hyperplasia. In this study, we examined the effects of hRAD50 on the morphological changes and migration of endothelial cells (EC) as possible mechanisms by which hRAD50 might block angiogenesis. Quantitative image analysis revealed significant inhibition of the number and total area of blood vessels in rat tumor tissues following hRAD50 gene delivery. hRAD50 distorted actin and tubulin arrangements, and significantly reduced the F/G-actin ratio and increased the nitric oxide (NO) production in the primary cultured human EC. These effects were blocked by pretreatment with L-NAME (N^G-nitro-L-arginine-methyl ester), a NO synthase inhibitor. FACScan analysis showed that NO was involved in the necrosis and apoptosis of EC by hRAD50. hRAD50 also inhibited EC migration in an in vitro wound-healing model. These results indicate that NO-dependent cytoskeletal changes and inhibition of EC migration contribute to the suppression of angiogenesis by hRAD50 delivery in vivo.
© 2003 Federation of European Biochemical Societies. Published by Elsevier B.V. All rights reserved.

Key words: RAD50; Endothelial cell; Angiogenesis; Nitric oxide; Migration; Actin

1. Introduction

Human RAD50 (hRAD50) is a nuclear protein that exhibits a limited degree of homology to chromosomal structural maintenance proteins and synaptonemal complex proteins [1], and has limited epitopic homology to p53 [2]. hRAD50 is part of a trimeric complex, hRAD50/MRE11/NBS1. This complex functions in DNA damage detection and repair. The hRAD50 is an abundant protein that is uniformly distributed in the nuclei of cultured cells. Following gamma irradiation, both hRAD50 and hMRE11 formed discrete nuclear foci, which

are referred to as ionizing radiation-induced foci, indicating that hRAD50 and hMRE11 exhibit a dynamic redistribution within the nucleus after treatment with agents that induce DNA double-strand break [3]. Recently, we observed that hRAD50 overexpression in cultured non-endothelial cells (non-EC) caused p21-caspase-dependent cell death [4]. We also showed that overexpression of hRAD50 in several cultured cells, such as HeLa and SaOS-2 cells, induced necrosis and apoptosis. We observed inducible nitric oxide synthase (iNOS) induction in the regressed tumor tissues when we injected the hRAD50 gene into subcutaneous adenocarcinoma in an experimental rat or mouse model. In vivo, hRAD50 gene delivery clearly had antitumor activity.

The mechanism of hRAD50's antitumor activity is unknown, but it appears to involve a reduction of angiogenesis through the activity of NO as well as p21-caspase-dependent direct cytotoxic action. In hRAD50-transfected tumor sections, there were fewer blood vessels than in the control section. Also, hRAD50 gene transfer caused deaths of cultured human coronary arterial EC (HCAEC) and human coronary arterial smooth muscle cells (HCASMC) [5]. Compared with non-EC, increased endothelial NO synthase (eNOS) expression as well as p21 expression was observed in the EC. NO production was significantly increased in the hRAD50 group compared with the vector group after transient transfection. The Western result that iNOS was not induced by hRAD50 indicated that the increased NO generation was derived from the eNOS activation by hRAD50. Pretreatment with NOS and pan-caspase inhibitors completely prevented EC death by hRAD50, indicating involvement of NO as well as caspase in the profound EC death in the static culture model. We also observed that local hRAD50 gene delivery could cause significant regression of preformed in-stent neointimal hyperplasia in porcine coronary arteries without apparent systemic toxicity [5].

The roles of NO in the cardiovascular system are complex and include vessel relaxation, inhibition of the proliferation of SMC and EC, and suppression of platelet adhesion [6]. The eNOS protein is constitutively expressed in myocardial cells as well as coronary EC, and has autocrine and paracrine actions on cardiomyocytes and vascular cells [7]. Induction of apoptosis by NO has been described in various cell lines [8,9], while some studies have demonstrated that NO inhibits apoptosis [10,11]. Thus, the role of NO in apoptosis appears to be cell-type specific. In EC, NO has both anti-apoptotic and pro-apoptotic effects depending on the NO concentration [12]. NO

*Corresponding author. Fax: (82)-62-232-6974.
E-mail address:* kimkk@chonnam.ac.kr (K.K. Kim).

reacts rapidly with superoxide to form the highly toxic peroxynitrite, and it has been demonstrated that both NO and peroxynitrite can damage DNA directly [13].

To investigate the possible mechanisms by which hRAD50 blocks angiogenesis, we studied the effects of transient hRAD50 gene transfer on the morphological phenotypes and migration of primary cultured HCAEC. HCAEC were chosen because it is difficult to maintain stable hRAD50 over-expression in primary cultured EC. Our present results suggest that EC-specific cytoskeletal changes and inhibition of EC migration as well as profound NO- and caspase-mediated EC death may be the underlying mechanisms that block angiogenesis and thereby cause regression of experimental tumors and neointimal hyperplasia following hRAD50 delivery.

2. Materials and methods

2.1. Generation of experimental rat tumor model and hRAD50 DNA injection into tumor

The rat tumor model was made by injecting 3×10^5 (50 μl) RBA cells subcutaneously in the right flanks of newborn (1∼2 days) Sprague–Dawley rats. The RBA cell was derived from rat mammary adenocarcinoma (ATCC, CRL-1747). After 4 weeks, a palpable tumor mass (diameter less than 1 cm) was confirmed and a gene expression cassette mixed with non-liposomal lipid FuGENE 6 (Boehringer Mannheim) was injected directly into the tumor mass. Rats were injected weekly, for 2 weeks, with a control pFLAG vector or pFLAG-hRAD50 DNA, and survival of the animals was monitored for 3∼6 months following gene injection.

2.2. Morphometric analysis of tumor vessels

Sections of rat subcutaneous tumors generated in a previous study [4] were stained with hematoxylin. Representative sections obtained from three tumors from each group (control and hRAD50-injected) were analyzed using a Nikon E-600 microscope. Images were captured with a Spot digital camera, and morphometric analyses were performed using Image-Pro Plus (Media Cybernetics) software. The whole field was examined at $200\times$ magnification on each cross-section, and the number of vessels per mm^2, the total area of tumor blood vessels, and the sectioned tumor area were determined. The Student's unpaired t-test was used to analyze differences in the vessel number and area.

2.3. Cell cultures

HCAEC and HCASMC were purchased from Clonetics at passage 3 and used until passage 8. These cells were grown in basic media (EBM2 for EC and SmBM2 for SMC; Clonetics) containing growth supplements (EGM2MV or SmGM2; Clonetics). HCT116 human colon cancer cells were cultured as described [4].

2.4. Construction of plasmids and transfection

Mammalian expression vector (pFLAG; Eastman Kodak) for hRAD50 and control CMV-β-gal vector (Clontech) were used as described [4]. DNA (2 μg) was transfected into 70% confluent cells in 1 ml of culture media with FuGENE 6 following the manufacturer's protocol. The transfection rate was measured by counting the stained cells with β-gal staining solution (Specialty Media). The average transfection rates of the HCAEC, HCASMC, and HCT116 cells were 16%, 24%, and 46%, respectively. In some experiments, 10^{-4} M N^G-nitro-L-arginine-methyl ester (L-NAME; Sigma) was added before transfection to block the activation of eNOS by hRAD50.

2.5. Fluorescent immunocytochemistry

Cells were seeded for confocal laser scanning microscopy, transfected with vector or hRAD50, washed, fixed, probed, visualized and observed as described [4]. For tubulin staining, monoclonal mouse anti-alpha tubulin antibody (1:100; Zymed) was used. The cells were visualized with Alexa Fluor 568-conjugated goat anti-mouse IgG (Molecular Probes; 1:500) in blocking solution for 30 min. The nucleus was then counterstained with Sytox Green (1 μmol, Molecular Probes) and observed with confocal laser scanning microscopy (Bio-Rad; 1024).

2.6. NO measurement

Forty-eight hours after the transfection with hRAD50, the media were collected and stored at $-80°C$. After converting nitrate into nitrite by nitrate reductase, the nitrite contents were measured with a Colorimetric NO assay kit (Oxford Biomedical Research) following the manufacturer's protocol.

2.7. Staining and quantitative measurement of F-actin and G-actin

The cells were fixed and permeabilized as described above [5]. If needed, L-NAME (10^{-4} M) was added before transfection to block the activation of eNOS by hRAD50. F-actin and G-actin were visualized by staining with Alexa Fluor 488-conjugated phalloidin and tetramethylrhodamine-conjugated DNase I, respectively, as described in the manufacturer's protocol (Molecular Probes). The cells were observed with confocal laser scanning microscopy.

F-actin and G-actin contents were measured by the methods of Howard and Oresajo [14]. The F-actin content was obtained from the absorbance at 518 nm and the G-actin content at 590 nm. The absorbance of each sample was measured six times for each sample and averaged. Each experiment was carried out in triplicate and two independent experiments were performed for each set of samples. To evaluate the effects of NO on the F/G-actin ratio, the cells were incubated with 50 μM S-nitroso-N-acetylpenicillamine (SNAP; Tocris Cookson) for 1 day, and the F/G ratio was measured.

2.8. Flow cytometry

hRAD50-transfected HCAEC suspensions with or without L-NAME (10^{-4} M) pretreatment before transfection were stained with propidium iodide and Annexin V-FITC (Boehringer Mannheim), and the status of cell death (two-dimensional FACScan) was measured with a FACScan flow cytometer (Becton Dickinson, Sunnyvale, CA, USA) using a Cycle Test PLUS DNA Reagent kit (Becton Dickinson).

2.9. In vitro wound-healing assay

The wound-healing assay was performed as described [15]. In brief, after HCAEC were grown to over-confluence in a six-well plate, a scratch was made using a sterile cell-scraper, and a starting point was marked by attaching a cover glass under the bottom of the plate. After fresh culture medium was supplied, the vector or hRAD50 was transfected as described above. The cells were incubated for 2 days, fresh medium supplied again, and the vector or hRAD50 was transfected again. After the cells were incubated for 2 days longer, cells that had migrated into the cell-free area were counted under inverted microscopy (magnification $\times 100$). The cells in the five small grids of an eyepiece micrometer [Olympus, unit area; 0.1 mm (height) $\times 0.5$ mm (width)] just above the starting point were counted and then the area next to the wound side was counted again. The number of cells per consecutive unit area were counted, and the process continued until no cells were observed. The cell counts were plotted using the consecutive field number as the abscissa, and both X- and Y-axis intercepts were calculated by extrapolating the regression line.

2.10. Statistical analysis

Results are expressed as mean ± S.E.M. The statistical significance of differences between the treatment groups was determined using ANOVA (analysis of variance) and Student's unpaired t-test. A value of $P < 0.05$ was considered statistically significant.

3. Results and discussion

3.1. Quantification of the effects of hRAD50 injection on tumor-induced angiogenesis in the rat tumor model

Previously, we reported that the subcutaneous tumor had regressed after 2 weeks following the second injection of hRAD50, and a complete regression of 14 from 18 established tumors was achieved within 1 week after the start of regression [4]. Here, we examined histological sections of tumors excised from rats injected with vector alone or hRAD50 [4]. The tumors were excised 2 weeks following the second injection. Microphotographs of hematoxylin-stained sections showed that proliferating adenocarcinoma cells were abun-
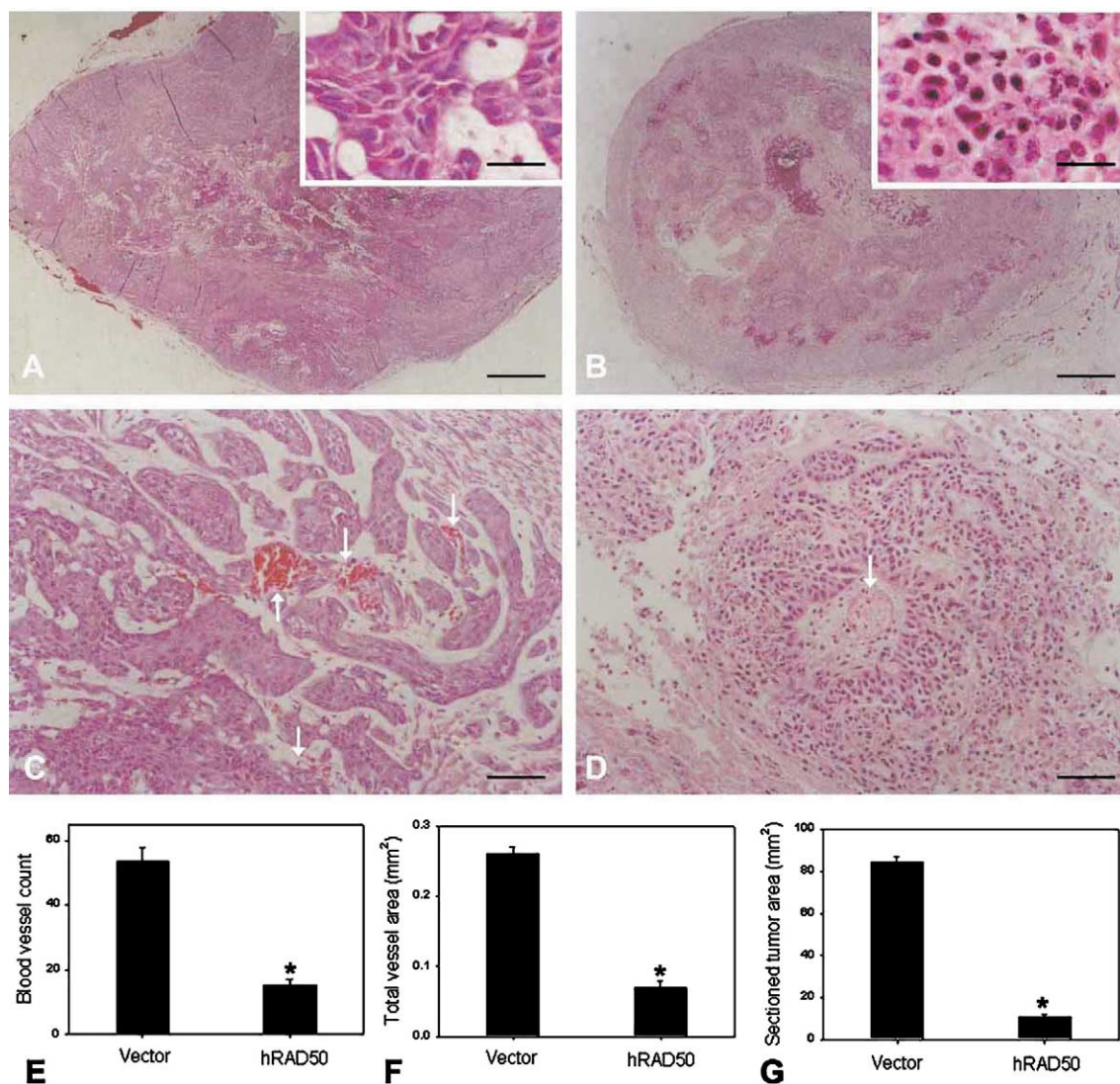
Fig. 1. The effect of hRAD50 gene delivery on tumor-induced angiogenesis. The subcutaneous adenocarcinoma tissues of rat given the vector alone or the hRAD50 expression cassette were analyzed by histology and image analysis. Representative hematoxylin-stained sections (A,B: low-power field; C,D: high-power field) are shown ($n = 3$). Proliferating cells were abundant (inset) in the vector-injected tumor sections (A). In the hRAD50-delivered tumor sections (B), tumor margins were well encapsulated and there were a lot of apoptotic cells in the regressed tumor tissue (inset). There were fewer blood vessels (arrows) in the hRAD50-delivered tumor sections (D) than in the vector-injected tumor sections (C). Quantitative computer-assisted image analysis revealed a significant inhibition of angiogenesis in the hRAD50 gene delivery group compared with the vector-injected group, as measured by the number of blood vessels (E) and total vessel area (F) per cross-sectional area. The relative tumor area was reduced seven-fold in the hRAD50 gene delivery group, as compared with the vector-injected group (G). Scale bar A, 1500 μm; B, 750 μm; inset, 37.5 μm; C,D, 75 μm.

dant in the vector-injected tumor section (Fig. 1A, inset). Also, there were many blood vessels in the tumor section (Fig. 1C). However, in the hRAD50-delivered tumor sections, tumor margins were well encapsulated (Fig. 1B) and there were fewer blood vessels (Fig. 1D). Also, there were a lot of apoptotic cells in the regressed tumor tissue (Fig. 1B, inset). To achieve a more detailed quantification of the effects of hRAD50 injection on tumor-induced angiogenesis, the total vessel number and vessel area per cross-sectional tumor area were determined by computer-assisted image analysis of representative digital images. Whereas control tumors demonstrated between 46 and 60 vessels per sectioned tumor area, the vessel number was significantly reduced by more than 70% in hRAD50-injected tumors (Fig. 1E). Also, the total vessel area was reduced by more than 70% in hRAD50-delivered

tumors as compared with control tumors (Fig. 1F). Likewise, the relative cross-sectioned tumor area was reduced by more than 80% in hRAD50-injected tumors (Fig. 1G).

3.2. hRAD50-induced cytoskeletal phenotypes

Since hRAD50 induces the enlargement of the cell and multinucleation [4], we speculated that the nuclear and cytoplasmic morphological changes induced by hRAD50 might be caused by changes in the cytoskeleton. The subtle changes of intracellular fibers could not be seen easily with regular fluorescent microscopy at low power (data not shown). Instead, confocal images with a higher magnification was used for showing the alterations. In control and vector-treated HCAEC, tubulin was arranged in a radial pattern from the nucleus to the periphery of the cytoplasm (Fig. 2A,B). How-
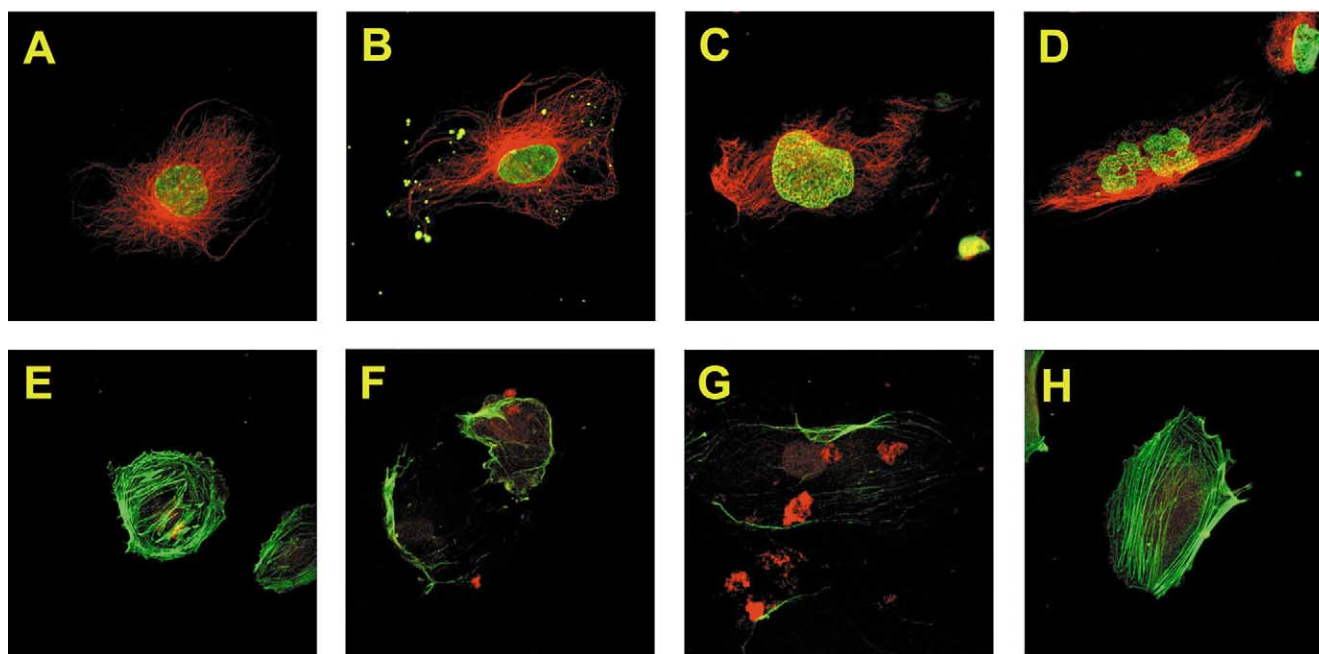
Fig. 2. hRAD50-induced changes in nuclear shape and microfilament arrangement. A–D: Tubulin of HCAEC was visualized. Control (A), vector-transfected cells (B), and hRAD50-transfected cells (C,D) are shown. Note that hRAD50 disturbs the arrangement of the tubulin (C), and causes multinucleation (D). E–H: F-actin and G-actin are visualized. Cells transfected with vector (E) or hRAD50 (F,G), or hRAD50 following L-NAME pretreatment (H) are represented. Note that the hRAD50 induced the disruption of the cell and distortion of F-actin (F). Some typical G-actin aggregates are shown (G). However, L-NAME prevented the disarray of F- and G-actin by hRAD50 (H). All magnifications: ×160.

ever, in the hRAD50-treated HCAEC, the nucleus was bizarre and divided (Fig. 2C,D). In addition, the arrangement of tubulin was disrupted and distorted (Fig. 2C,D).

In the control and vector-treated groups, F-actin ran from the edge of one end of the cytoplasm to the opposite side, and showed a continuous filamentous shape, while the G-actin was localized near the nucleus (Fig. 2E). However, after hRAD50 transfection, the actin fiber arrangement was significantly changed. The arrangement of the F-actin was severely disrupted and the amount was reduced (Fig. 2F). Interestingly, the G-actin was clustered near the nucleus or in the cytoplasm (Fig. 2G). However, when the cells were pretreated with L-NAME, the actin arrangement was not disrupted (Fig. 2H). Thus, NO seems to be related to the distorted actin arrangement in EC transformed with hRAD50.

3.3. Measurement of NO contents in the media and effect of NO on actin content

We measured NO content in the medium as nitrite after transient transfection with either vector or hRAD50. NO production was significantly increased in the hRAD50 group (1.90 ± 0.55 nmol per 10 000 cells) compared with the vector group (0.36 ± 0.05) at 48 h after transient transfection (Fig. 3A, $P < 0.05$). The amount of NO produced is equivalent to 4 µM in our study. It is unlikely that the amount of 4 µM is sufficient to induce the apoptosis instead of cell proliferation. However, due to the paracrine or autocrine nature of released NO, the total concentration in the medium may not reflect the fine intracellular NO contents, which is sufficient to cause any significant changes. Indeed, when the endogenous NO is induced by exogenous stimulant such as humic acid, even 400 pmol per 10 000 cells, an amount of 1/5 of our results, is sufficient to fully induce the apoptosis in human EC [16].

Also, with pretreating with L-NAME, the NO level (0.42 ± 0.06) was decreased to the vector-treated level (0.31 ± 0.05), indicating that the increased NO contents by hRAD50 transfection are completely blocked by the treatment of NOS inhibitor (Fig. 3A).

Previously, we observed that hRAD50 gene transfer increased eNOS expression in the cultured EC and eNOS staining in the hRAD50-delivered coronary arteries, but iNOS was not expressed in control or gene-delivered coronary arteries [5]. However, it was reported that iNOS could be induced in the EC [17], suggesting the possible involvement of iNOS in the endothelial homeostasis. Indeed, to address whether the increased NO release by hRAD50 is derived from eNOS or iNOS, we have conducted immunoblot with iNOS, but could not see any changes in iNOS expression (data not shown). Thus, the increased NO release in the EC by RAD50 seems to be derived from eNOS activation, however, it does not mean that iNOS can be completely ruled out in our model.

Since the actin antibody non-specifically binds to F-actin and G-actin, we adopted, instead of Western blot, a fluorescent quantification of F-actin and G-actin using fluorescent phalloidin and DNase I, respectively. The F/G-actin ratio was approximately 2:1 in the vector-transfected HCAEC. Although the magnitude of changes was small due to transient transfection, the ratio was significantly reduced in the hRAD50-treated group ($P < 0.01$, Fig. 3B). Interestingly, treatment with L-NAME blocked the changes in the F/G-actin ratio in the hRAD50-treated HCAEC (Fig. 3B). However, in non-endothelial HCT116 cells in which the eNOS expression is much lower than in the EC, hRAD50 transfection did not affect the F/G ratio (Fig. 3C), indicating that the hRAD50-induced change is specific to EC and suggesting that this change in the F/G ratio is not simply a feature of dying cells.
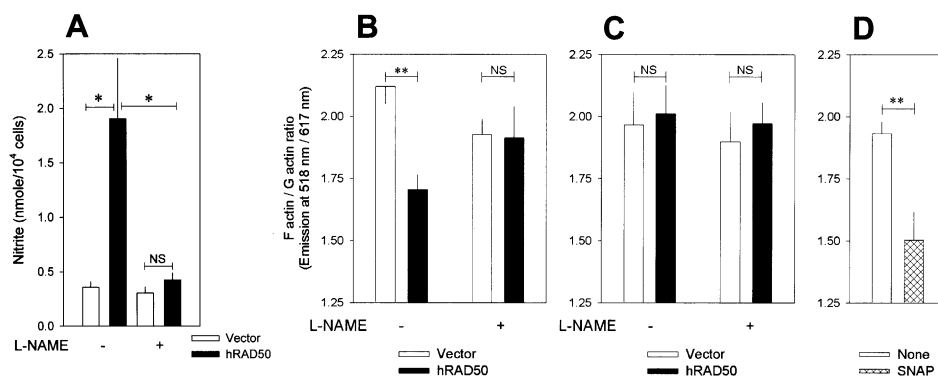
Fig. 3. Measurements of NO and F/G-actin contents. A: The NO contents were measured after forced expression of vector or hRAD50 with or without L-NAME pretreatment. hRAD50 significantly increases the amount of NO in the culture media compared with the vector-transfected group. The treatment with L-NAME lowers NO production by hRAD50 approximately to the level of untreated controls. There was significant difference in the NO level between the L-NAME-untreated and L-NAME-treated groups. B: The F-actin and G-actin of the transfected cells were simultaneously stained. In HCAEC, hRAD50 markedly decreased the F/G-actin ratio, while this decrease was completely blocked by pretreatment with L-NAME. C: hRAD50 failed to alter the F/G-actin ratio in HCT116 cells, non-EC. D: The hRAD50-induced effect on the F/G-actin ratio was simulated by treatment with SNAP, a NO donor. Asterisks indicate the significant differences between the hRAD50- and vector-transfected groups or by L-NAME treatment (*$P < 0.05$, **$P < 0.01$; NS, not significant).

To further examine whether NO is ultimately responsible for the changes in the F/G ratio in HCAEC, we simulated the effects of transient hRAD50 transfection with the NO donor SNAP. We used a low concentration of SNAP (50 µM) because that is sufficient to mimic the maximal activation of eNOS, which is considered to be equivalent to 1–50 µM of NO donors. SNAP also significantly reduced the F/G ratio in the HCAEC (Fig. 3D), indicating that NO mediates the change in this ratio.

It was reported that gingival epithelial cells exposed to SNAP exhibited nuclear aberrations, including multilobed nuclei and multinucleation [9]. SNAP-induced cell death was apparently by apoptosis and correlated with the liberation of NO. Expression of the human eNOS gene in vivo suggests that NO or its toxic metabolite caused myocardial degradation, a part of which was compatible with apoptosis of the transfected cardiomyocytes themselves and the adjacent cells as a paracrine effect [18]. Also, unique cell degenerations by overexpression of the eNOS gene were ameliorated by L-NAME pretreatment. Previously, we observed that hRAD50 in non-EC resulted in cell death, followed by the appearance of multinucleated giant cells, and these processes were p21 dependent [4]. Other studies have also found that p21 overexpression led to abnormal mitosis and endoreduplication in recovering cells [19,20]. Taken together, these reports suggest that NO and p21 mediate multinucleation and cytoskeletal distortion in EC by hRAD50.

Different levels of NO may produce different effects on cells. NO donors, such as SNAP, *S*-nitroso-glutathione, spermine NONOate and *S*-nitrosocaptopril inhibit EC and SMC proliferation in a concentration-dependent manner [21–23]. Diethylamine NONOate caused concentration-dependent inhibition of EC DNA synthesis, which was reversed by the NO antagonist, cPTIO [22]. SNAP inhibited FGF2-induced neovascularization in the mouse Matrigel implant model [24]. The level of NO produced by inhibitory concentrations of SNAP was similar to the NO levels produced by the induction of iNOS in SMC. Also, NO derived endogenously from iNOS inhibits proliferation of murine EC lines [25]. However, it was reported that a low concentration of SNAP inhibited TNFα-induced endothelial apoptosis partly through the cGMP path-

way, whereas a high SNAP concentration induced endothelial apoptosis via cGMP-independent pathways [26]. These reports indicate that a low basal level of NO, produced under physiological conditions, might contribute to human EC survival through anti-apoptotic effects, whereas a high level of NO released under pathologic conditions or exogenous gene transfections might be cytotoxic to EC. Thus, hRAD50 gene transfer may be useful for the inhibition of neovascularization associated with cell proliferation due to NO donors.

3.4. NO is involved in necrosis and apoptosis induced by hRAD50

We investigated the characteristics of cell death in the transient hRAD50-transfected group by examining a two-dimensional FACScan. hRAD50 transfection increased the frequency of apoptosis ($10.05 \pm 0.43\%$ versus $23.31 \pm 3.23\%$, $P < 0.01$) and necrosis ($5.36 \pm 0.44\%$ versus $14.92 \pm 2.22\%$, $P < 0.01$) (Fig. 4B) compared with the vector-treated group (Fig. 4A), indicating that apoptosis and necrosis both contributed to the death of hRAD50 overexpressing cells.

We also examined the effect of L-NAME on cytotoxicity with two-dimensional FACScan in order to elucidate whether NO is related to the necrosis and/or apoptosis induced by hRAD50 (Fig. 4C,D). When compared with the untreated group (Fig. 4B), the apoptotic fraction induced by hRAD50 was significantly reduced from $23.3 \pm 3.2\%$ to $8.6 \pm 0.3\%$ in the L-NAME-pretreated group (Fig. 4D). However, even when L-NAME treatment was given, hRAD50 gene transfer still significantly increased apoptosis from $5.9 \pm 0.7\%$ to $8.6 \pm 0.3\%$ (Fig. 4D, $P < 0.05$) when compared with the vector group (Fig. 4C). Interestingly, in the case of necrosis, L-NAME blocked the increase in necrosis induced by hRAD50 ($9.30 \pm 0.22\%$ versus $10.05 \pm 1.22\%$, Fig. 4D). We represented the cell death in the hRAD50-transfected group and L-NAME-mediated alteration in cytotoxicity with changes of the fraction of hRAD50 transfection to that of vector transfection group (Fig. 4E). It showed that the apoptotic fraction induced by hRAD50 was significantly diminished by L-NAME pretreatment ($2.32 \pm 0.32\%$ versus $1.46 \pm 0.05\%$), but L-NAME blocked the increased necrosis induced by hRAD50 ($2.78 \pm 0.41\%$ versus $1.08 \pm 0.13\%$). Though the
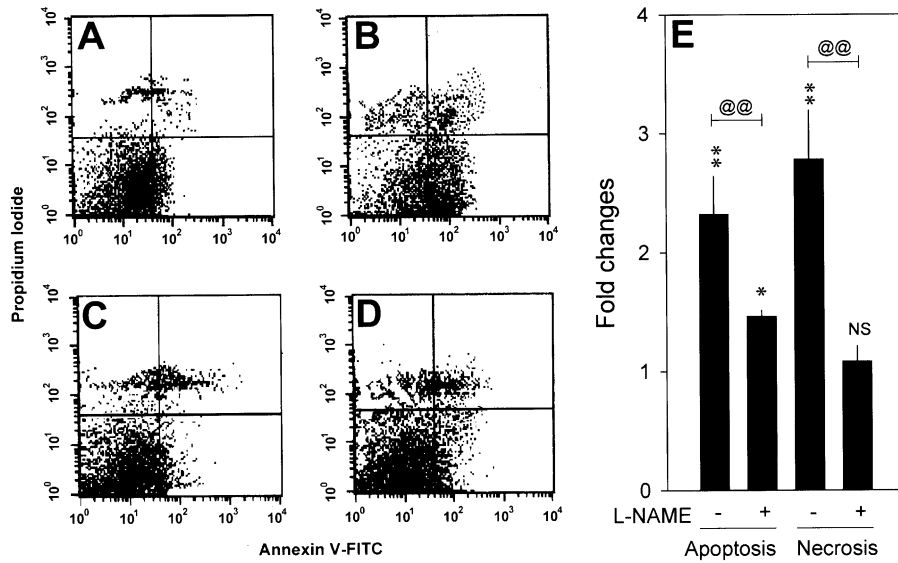
Fig. 4. FACScan analysis of hRAD50-transfected HCAEC. Two-dimensional analysis showed that apoptosis (lower right quadrant) and necrosis (upper right quadrant) were augmented in the hRAD50 group (B) compared with the vector group (A). L-NAME pretreatment was given in the vector- (C) and hRAD50-transfected groups (D). E: The apoptotic and necrotic fractions after hRAD50 transfection were divided by the mean apoptotic and necrotic fraction values of the vector-treated group, respectively, and expressed with fold changes. The asterisks indicate the statistical significances from their vector-treated control groups, while the @ signs show the differences between the L-NAME-treated and non-treated group (*$P < 0.05$, **$P < 0.01$; @$P < 0.05$, @@$P < 0.01$; NS, not significant). The apoptotic fraction induced by hRAD50 was significantly diminished by L-NAME pretreatment, but L-NAME blocked the increased necrosis by hRAD50, suggesting that NO mediates both mechanisms of cell death.

magnitudes of changes induced by hRAD50 were small due to transient transfection, these results suggest that NO mediates both mechanisms of cell death.

3.5. hRAD50 inhibits EC migration in a wound-healing model

Because hRAD50 induced cytoskeletal differentiated phenotypes in HCAEC, we used a wound-healing model to test whether these phenotypes might cause an attenuation of cell motility and EC migration (Fig. 5A). hRAD50 reduced the total cell number in the wound area (Fig. 5C, 63.5 ± 3.4) compared with the vector group (Fig. 5B, 128.0 ± 12.3, $P < 0.01$, $n = 6$), and decreased the *X*-intercept significantly (Fig. 5D, 6.3 ± 0.2 versus 5.5 ± 0.2, $P < 0.05$). Thus, the migrating capability of hRAD50-transfected cells was reduced. hRAD50 also decreased the *Y*-intercept markedly (Fig. 5D, 47.4 ± 3.6 versus 25.8 ± 1.3, $P < 0.01$, $n = 6$), indicating a decreased cell density at the wound-starting point.

EC migration is an important event in both physiological and pathological processes of angiogenesis, and is associated
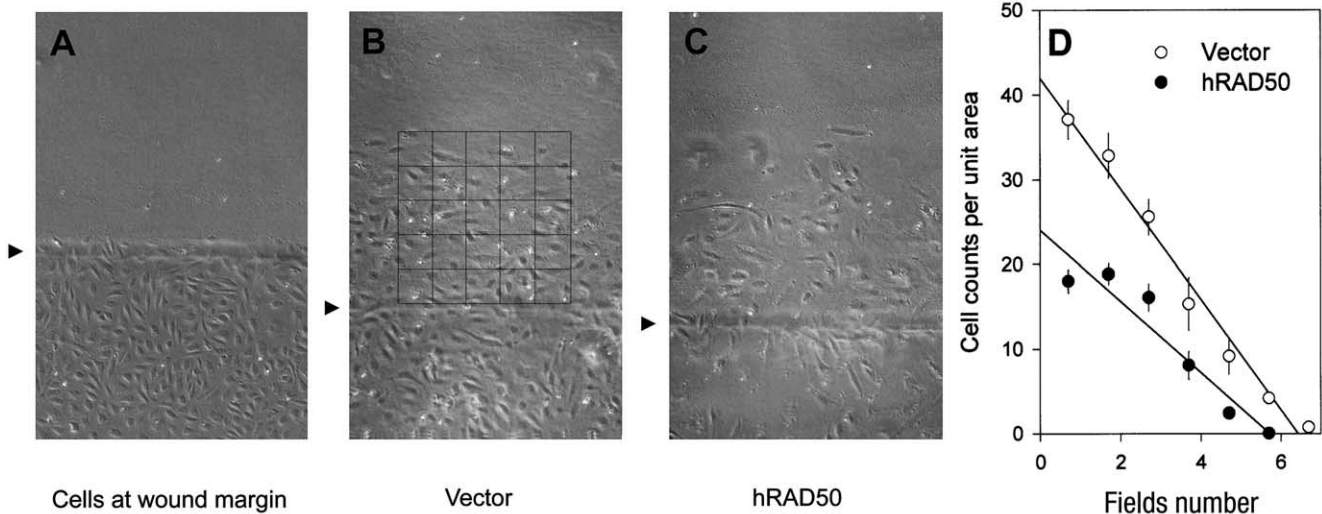

Fig. 5. Wound-healing assay showing the effects of hRAD50 transfection on the proliferation and lateral migration of HCAEC. A: Cells were scraped out and the wound-starting point was marked with a cover slide as indicated with an arrow. B: Four days after vector transfection, cells had migrated and proliferated in the cell-free area. EC per unit area were counted using an eyepiece micrometer. C: Effects of hRAD50 transfection on EC migration and proliferation. hRAD50 reduced the total EC number in the wound area (C) compared with the vector-treated group (B). D: Interpretation showing the extent of migration and proliferation of the hRAD50-transfected EC.

with regulation of the actin cytoskeleton. SNAP was reported to inhibit the serum-induced migration of cultured human umbilical vein EC in a time- and dose-dependent manner. Sodium nitroprusside also exhibited an antimigratory effect and superoxide dismutase, a NO protector, enhanced the antimigratory effect. Meanwhile, hemoglobin, a NO scavenger, eliminated the effect. These results indicated that antimigratory effect of SNAP was attributed to NO [27]. Statins, inhibitors of 3-hydroxy-3-methyl-glutaryl-coenzyme-A reductase, block angiogenesis by decreasing EC locomotion. Their effect is mainly caused by delocalization of RhoA from the cell membrane to the cytoplasm, thus disorganizing actin stress fibers [28]. This antiangiogenic activity could explain the beneficial effect of statins on cancer prevention [29]. Our results indicate that NO donors and hRAD50 inhibit EC migration through NO-mediated actions, and that statins and hRAD50 inhibit EC migration through disorganization of actin. Thus, this suggests that hRAD50 inhibits EC migration through NO-mediated disorganization of actin, and that hRAD50 and statins could be used in localized tumor gene therapy.

Based on our previous in vivo results from hRAD50 gene injection into tumor tissue and in vitro results showing profound EC death in a static culture system, we previously tested the effect of local delivery of the hRAD50 gene into the stent implantation site with a Dispatch catheter [5]. We hoped to enhance the cytotoxicity in EC by increased production of NO through eNOS activation as well as to reduce the proliferation of EC and SMC through caspase activation. Indeed, we observed significant regression of preformed in-stent neointimal hyperplasia after one-time local delivery of the hRAD50 gene [5]. Our present results provide in vitro evidence to shed light on the possible underlying mechanisms for how hRAD50 blocks angiogenesis, and confirm the potential utility of hRAD50 in local gene therapy against proliferative disorders, such as tumors and coronary restenosis.

References

[1] Dolganov, G.M., Maser, R.S., Novikov, A., Tosto, L., Chong, S., Bressan, D.A. and Petrini, J.H.J. (1996) Mol. Cell. Biol. 16, 4832–4841.

[2] Kim, K.K., Daud, A.I., Wong, S.C., Pajak, L., Tsai, S-C., Wang, H., Henzel, W.J. and Field, L.J. (1996) J. Biol. Chem. 271, 29255–29264.

[3] Maser, R.S., Monsen, K.J., Nelms, B.E. and Petrini, J.H. (1997) Mol. Cell. Biol. 17, 6087–6096.

[4] Shin, B.A., Ahn, K.Y., Kook, H., Koh, J.T., Kang, I.C., Lee, H.C. and Kim, K.K. (2001) Cell Growth Differ. 12, 243–254.

[5] Ahn, Y.K., Kook, H., Jeong, M.H., Ahn, K.Y., Cho, J.G., Park, J.C., Kang, J.C. and Kim, K.K. (2003) J. Gene Med. 5, in press.

[6] Vane, J.R., Anggard, E.E. and Botting, R.M. (1990) N. Engl. J. Med. 323, 27–36.

[7] Balligand, J.L., Kobzik, L., Hant, X., Kaye, D.M., Belhassent, L., O'Hara, D.S., Kelly, R.A., Smith, T.W. and Michel, T. (1995) J. Biol. Chem. 270, 14582–14586.

[8] Messmer, U.K., Reimer, D.M., Reed, J.C. and Brune, B. (1996) FEBS Lett. 384, 162–166.

[9] Babich, H., Zuckerbraun, H.L., Hirsch, S.T. and Blau, L. (1999) Pharmacol. Toxicol. 84, 218–225.

[10] Mannick, J.B., Miao, X.Q. and Stamler, J.S. (1997) J. Biol. Chem. 272, 24125–24128.

[11] Melino, G., Catani, M.V., Corazzari, M., Guerrieri, P. and Bernassola, F. (2000) Cell. Mol. Life Sci. 57, 612–622.

[12] Dimmeler, S. and Zeiher, A.M. (1999) Cell Death Differ. 6, 964–968.

[13] Brune, B., Mohr, S. and Messmer, U.K. (1996) Rev. Physiol. Biochem. Pharmacol. 127, 1–30.

[14] Howard, T.H. and Oresajo, C.O. (1985) J. Cell Biol. 101, 1078–1085.

[15] Kook, H., Itoh, H., Choi, B.S., Sawada, N., Doi, K., Hwang, T.J., Kim, K.K., Arai, H., Baik, Y.H. and Nakao, K. (2003) Am. J. Physiol. Heart Circ. Physiol. 284, H1388–H1397.

[16] Hseu, Y.C., Wang, S.Y., Chen, H.Y., Lu, F.J., Gau, R.J., Chang, W.C., Liu, T.Z. and Yang, H.L. (2002) Free Radic. Biol. Med. 32, 619–629.

[17] Zulueta, J.J., Sawhney, R., Kayyali, U., Fogel, M., Donaldson, C., Huang, H., Lanzillo, J.J. and Hassoun, P.M. (2002) Am. J. Respir. Cell Mol. Biol. 26, 22–30.

[18] Kawaguchi, H., Shin, W.S., Wang, Y., Inukai, M., Kato, M., Matsuo-Okai, Y., Sakamoto, A., Uehara, Y., Kaneda, Y. and Toyo-oka, T. (1997) Circulation 95, 2441–2447.

[19] Bates, S., Ryan, K.M., Phillips, A.C. and Vousden, K.H. (1998) Oncogene 17, 1691–1703.

[20] Chang, B.D., Broude, E.V., Fang, J., Kalinichenko, T.V., Abdryashitov, R., Poole, J.C. and Roninson, I.B. (2000) Oncogene 19, 2165–2170.

[21] Cornwell, T.L., Arnold, E., Boerth, N.J. and Lincoln, T.M. (1994) Am. J. Physiol. 267, C1405–C1413.

[22] Sarkar, R., Webb, R.C. and Stanley, J.C. (1995) Surgery 118, 274–279.

[23] Jia, L., Wu, C.C., Guo, W. and Young, X. (2000) Eur. J. Pharmacol. 391, 137–144.

[24] Powell, J.A., Mohamed, S.N., Kerr, J.S. and Mousa, S.A. (2000) J. Cell. Biochem. 80, 104–114.

[25] Cartwright, J.E., Johnstone, A.P. and Whitley, G.S. (2000) Br. J. Pharmacol. 131, 131–137.

[26] Shen, Y.H., Wang, X.L. and Wilcken, D.E. (1998) FEBS Lett. 433, 125–131.

[27] Lau, Y.T. and Ma, W.C. (1996) Biochem. Biophys. Res. Commun. 221, 670–674.

[28] Vincent, L., Chen, W., Hong, L., Mirshahi, F., Mishal, Z., Mirshahi-Khorassani, T., Vannier, J., Soria, J. and Soria, C. (2001) FEBS Lett. 495, 159–166.

[29] Brower, V. (2003) J. Natl. Cancer Inst. 95, 844–846.